Eur. Phys. J. Plus (2017) **132**: 96
DOI 10.1140/epjp/i2017-11361-8

THE EUROPEAN PHYSICAL JOURNAL PLUS

Regular Article

Numerical investigation of velocity slip and temperature jump effects on unsteady flow over a stretching permeable surface

E. Hosseini[1,a], G.B. Loghmani[1,b], M. Heydari[1,c], and M.M. Rashidi[2,3,d]

[1] Department of Mathematics, Yazd University, Yazd, Iran
[2] Shanghai Key Lab of Vehicle Aerodynamics and Vehicle Thermal Management Systems, Tongji University, 4800 Cao An Rd., Jiading, Shanghai 201804, China
[3] ENN-Tongji Clean Energy Institute of Advanced Studies, Shanghai, China

Received: 19 August 2016 / Revised: 13 January 2017
Published online: 24 February 2017 –

Abstract. In this paper, the boundary layer flow and heat transfer of unsteady flow over a porous accelerating stretching surface in the presence of the velocity slip and temperature jump effects are investigated numerically. A new effective collocation method based on rational Bernstein functions is applied to solve the governing system of nonlinear ordinary differential equations. This method solves the problem on the semi-infinite domain without truncating or transforming it to a finite domain. In addition, the presented method reduces the solution of the problem to the solution of a system of algebraic equations. Graphical and tabular results are presented to investigate the influence of the unsteadiness parameter A, Prandtl number Pr, suction parameter f_w, velocity slip parameter γ and thermal slip parameter ϕ on the velocity and temperature profiles of the fluid. The numerical experiments are reported to show the accuracy and efficiency of the novel proposed computational procedure. Comparisons of present results are made with those obtained by previous works and show excellent agreement.

Nomenclature

$B_{i,n}(x)$	Bernstein polynomial of degree n
$\mathfrak{B}_{i,n}(x)$	Orthogonal Bernstein polynomial of order n
$\bar{\mathfrak{B}}_{i,n}(x)$	Orthonormal Bernstein polynomial of order n
$\mathbb{B}_n f(t)$	Bernstein function of order n
t	Time (s)
x, y	Cartesian coordinates along the surface and normal to it, respectively (m)
$u_w(x,t)$	Sheet stretching velocity (m s^{-1})
u, v	Velocity component in the x- and y-directions (m s^{-1})
a, c	Constants (s^{-1})
b	Constant (K m^{-1})
$v_w(x,t)$	Sheet stretching mass transfer (m s^{-2})
T	Temperature of the fluid (K)
L_1	Velocity slip factor (m^{-1} s)
M_1	Thermal slip factor (m)
T_w	Wall temperature (K)
T_∞	Ambient temperature (K)
Pr	Prandtl number
A	Unsteadiness parameter
f_w	Velocity ratio parameter
C_f	Skin friction coefficient
Nu_x	Local Nusselt number
q_w	Local heat flux form the sheet (W m^{-2})
k	Thermal conductivity (W m^{-1} K)
Re_x	Local Reynolds number

Greek symbols

ν	Kinematic viscosity (m^2 s^{-1})
α	Thermal diffusivity (m^2 s^{-1})
γ	Dimensionless velocity slip parameter
φ	Dimensionless thermal slip parameter
τ_w	Skin fraction (Pa)
μ	Dynamic viscosity (kg m^{-1} s^{-1})
ρ	Fluid density (kg m^{-3})

[a] e-mail: ehsanhoseini66@gmail.com
[b] e-mail: loghmani@yazd.ac.ir
[c] e-mail: m.heydari@yazd.ac.ir (corresponding author)
[d] e-mail: mm_rashidi@tongji.edu.cn

1 Introduction

The boundary layer flow past a stretching plate was first dealt with Crane [1], who solved analytically the steady two-dimensional flow past a linearly stretching plate. This phenomenon has many important applications in engineering processes, such as manufacture of foods, glass fibre and paper production, drawing of plastic films and wires, crystal growing, polymer extrusion and liquid films in condensation process. Several of research papers on a stretching sheet have been published by considering different parameters like viscous dissipation, radiation effect, magnetic field, suction/injection, slip effect and heat generation/absorption with various types of fluids like viscoelastic fluid, micropolar fluid and nanofluid. Gupta *et al.* [2] extended the problem of fluid flow past a stretching surface, in case of moving boundary flow, to a permeable surface that important in extrusion processes. Ishak *et al.* [3] studied the unsteady laminar boundary layer flow over a continuously stretching permeable surface. Abolbashari *et al.* [4] used homotopy analysis method (HAM) to study the entropy analysis in an unsteady magnetohydrodynamic (MHD) nanofluid regime adjacent to an accelerating stretching permeable surface. Rashidi *et al.* [5] proposed the homotopy simulation of nanofluid dynamics from a nonlinearly stretching isothermal permeable sheet with transpiration. Freidoonimehra *et al.* [6] investigated the transient MHD laminar free convection flow of nanofluid past a permeable stretching vertical surface.

In fluid dynamics, the no-slip boundary condition happens when liquid adheres to a solid boundary. It is noticed that, the behavior of fluids with micro-scale dimensions varies from the traditional fluid flow and depends to the slip flow regime. So, the no-slip condition is inadequate when the fluid is particulate, such as suspensions, emulsions, foams and polymer. Also, the fluid flow in many applications of micro/nano systems like micro-valve, hard disk drive, micro-nozzles, micro-pump and micro-electro-mechanical systems (MEMS) is in slip regime, which is specified by slip boundary condition. Although the no-slip boundary condition is known as the main appearance of the Navier-Stoke's theory, the slip flow motion still obeys the Navier-Stoke's equations but with slip velocity and temperature conditions. Maxwell [7] introduced the slip velocity for rarefied gases flowing over a solid surface. Thompson proposed a second-order slip model, based on Maxwell's first-order slip model. The many investigators reported that Thompson's model cannot estimate the flow in high Knudsen number (Kn). Beskok *et al.* [8] presented an improved second-order slip condition. For more details, see [9,10].

Despite many studies on a stretching sheet, the researches on the boundary layer flow over a stretching sheet is limited to some fluids flow with traditional no-slip flow boundary condition and a little attention was given to stretching sheet with slip boundary condition. Andersson [11] investigated slip flow past a stretching surface. He considered a closed form solution of a full Navier-Stoke's equations for a MHD flow over a stretching sheet. Wang [12] presented the exact solution of a full Navier-Stoke's equations base of Anderson's solution for the flow due to a stretching sheet with partial slip. Fang *et al.* [13] suggested slip magnetohydrodynamic viscous flow over a permeable shrinking sheet. Hayat *et al.* [14] analyzed MHD flow and heat transfer over permeable stretching sheet with slip conditions. Jafari *et al.* [15] presented the second law of thermodynamics over a stretching permeable surface in the presence of the uniform vertical magnetic field in the slip nanofluid regime. Abolbashari *et al.* [16] provided analytical modeling of entropy generation for Casson nanofluid flow induced by a stretching surface in the presence of velocity slip and convective surface boundary conditions.

Currently, Nawaz *et al.* [17] have studied the Joules heating effects on stagnation point flow of Newtonian and non-Newtonian fluids over a stretching cylinder by means of genetic algorithm (GA). The effect of thermal radiation and heat transfer on the flow of ferromagnetic fluid on a stretching sheet is investigated in [18]. In [19], the unsteady boundary layer flow ferromagnetic fluid and heat transfer past a stretching surface with the influence of magnetic dipole are considered and solved numerically by employing shooting based RKF-45 method. The Falkner-Skan boundary layer steady flow over a flat stretching sheet was analyzed by Maqbool *et al.* [20]. A theoretical study of the problem of the peristaltic flow of Jeffrey fluid in a non-uniform rectangular duct under the effects of Hall and ion slip was established by Ellahi *et al.* [21]. Ellahi and Hussain [22] have studied the closed-form solutions of peristaltic flow of Jeffery fluid under the simultaneous effects of magnetohydrodynamics (MHD) and partial slip conditions in a rectangular duct.

Bernstein polynomials have important applications in computer graphics and have been applied for approximations of functions in many areas of mathematics and other fields such as smoothing in statistics and constructing Bézier curves [23–25]. These polynomials were first used by Sergei Natanovich Bernstein in a constructive proof for the Stone-Weierstrass approximation theorem. Bernstein polynomials have been applied to solve various kinds of ordinary and partial differential equations, integral equations and integro-differential equations defined in engineering and science [26–39]. Recently, Heydari *et al.* [25] applied the Gram-Schmidt orthogonalization process to find orthogonal Bernstein polynomials for the solution of heat transfer of a micropolar fluid through a porous medium with radiation.

The aim of the present work is study an unsteady flow past a permeable stretching sheet in the presence of the velocity slip and temperature jump effects. The governing nonlinear ordinary differential equations are solved numerically by using a new collocation method based on rational Bernstein polynomials. Motivated by this fact, present work analyzes the effects of the unsteadiness parameter, Prandtl number, suction parameter, velocity slip parameter and thermal slip parameter on the fluid velocity and temperature distribution profiles.

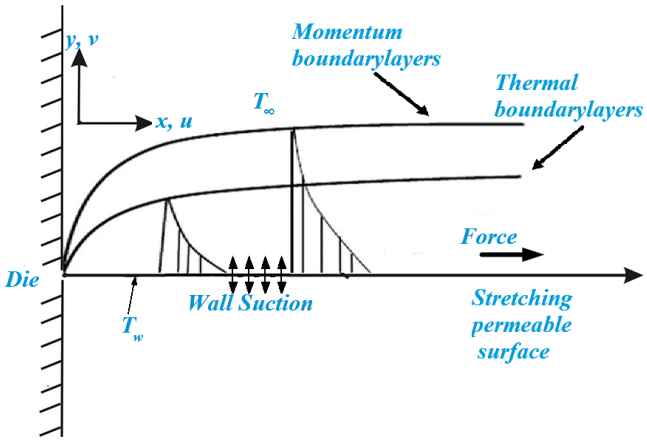

Fig. 1. Physical model and coordinate system.

This paper is organized as follows: In sect. 2, the mathematical formulation of an unsteady flow past a porous accelerating stretching surface in the presence of the velocity slip and temperature jump effects is presented. In sect. 3, we give some preliminaries and drive some tools for developing our method. A collocation method for solving the governing equations based on rational Bernstein functions is proposed in sect. 4. The results and discussion for the all values of the relevant parameters are presented in sect. 5. Finally, in sect. 6, some conclusions are provided.

2 Problem statement and mathematical modelling

Consider a two-dimensional laminar flow of an incompressible viscous fluid over an accelerating stretching permeable surface in the presence of the velocity slip and temperature jump effects. The geometry and coordinate systems of the problem are shown in fig. 1. The flow motion is assumed to be in the x- and y-directions, which are taken along and perpendicular to the plate, respectively. Also, the flow is confined over the region of $y > 0$. We assume that the unsteady fluid and heat flows start at time $t = 0$ and for time $t < 0$ they are steady. Moreover, the sheet is being stretched with the velocity $u_w(x,t)$ along the x-axis as

$$u_w(x,t) = \frac{ax}{1-ct}\,, \tag{1}$$

where $a > 0$ and $c \geq 0$ are constants with $ct < 1$, and both have dimension $(\text{time})^{-1}$. Further, $v_w(t)$ is the velocity of the mass transfer perpendicular to the stretching surface that defines as below:

$$v_w(t) = \frac{v_0}{\sqrt{1-ct}}\,. \tag{2}$$

Under these assumptions, by using the boundary layer approximations, the governing equations for mass, momentum and temperature can be written in the usual notations as [40]

$$\frac{\partial u}{\partial x} + \frac{\partial v}{\partial y} = 0, \tag{3}$$

$$\frac{\partial u}{\partial t} + u\frac{\partial u}{\partial x} + v\frac{\partial u}{\partial y} = \nu\frac{\partial^2 u}{\partial y^2}\,, \tag{4}$$

$$\frac{\partial T}{\partial t} + u\frac{\partial T}{\partial x} + v\frac{\partial T}{\partial y} = \alpha\frac{\partial^2 T}{\partial y^2}\,, \tag{5}$$

where u and v are the velocity components of the fluid along the x- and y-directions, respectively, α is the thermal diffusivity, T is the temperature of the fluid and ν is the kinematic viscosity.

The corresponding boundary conditions with partial slip for the velocity and the temperature are given by

$$u = u_w(x,t) + L_1\nu\frac{\partial u}{\partial y}\,, \quad v = v_0(t), \quad T = T_w(x,t) + M_1\frac{\partial T}{\partial y}\,, \quad \text{at } y = 0, \tag{6}$$

$$u \to 0, \quad T \to T_\infty, \quad \text{as } y \to \infty, \tag{7}$$

where $M_1 = M\sqrt{1-ct}$ is the thermal slip factor and $L_1 = L\sqrt{1-ct}$ is the velocity slip factor, M and L are the initial values of thermal and velocity slip factors, respectively, T_∞ is the ambient temperature and $T_w(x,t)$ is the temperature of the wall. The temperature function $T_w(x,t)$ not only has a linear variation with x but also has an inverse square law for its decrease with time in the following form:

$$T_w(x,t) = T_\infty + \frac{bx}{(1-ct)^2}\,, \tag{8}$$

where b is a constant, with $b<0$ and $b>0$ corresponding to the opposing and assisting flows, respectively, and $b=0$ is for the forced convection limit.

According to Freidoonimehr *et al.* [40], we introduce the following dimensionless functions $f(\eta)$ and $\theta(\eta)$, and the similarity variable η:

$$\eta = \left(\frac{a}{\nu(1-ct)}\right)^{1/2} y, \qquad \psi = \left(\frac{\nu a}{1-ct}\right)^{1/2} x f(\eta), \qquad \theta(\eta) = \frac{T-T_\infty}{T_w - T_\infty}\,, \tag{9}$$

where $\psi(x,y,t)$ is a stream function defined as

$$u = \frac{\partial \psi}{\partial y} = \frac{ax}{1-ct} f'(\eta), \tag{10}$$

$$v = -\frac{\partial \psi}{\partial x} = -\left(\frac{\nu a}{1-ct}\right)^{1/2} f(\eta), \tag{11}$$

which identically satisfies the mass conservation equation (3). Substituting the above similarity transformations into (4)–(7), we obtain the following system of nonlinear ordinary differential equations:

$$f'''(\eta) - f'(\eta)^2 + f(\eta) f''(\eta) - A\left(f'(\eta) + \frac{1}{2}\eta f''(\eta)\right) = 0, \tag{12}$$

$$\frac{1}{Pr}\theta''(\eta) + \begin{vmatrix} f(\eta) & \theta(\eta) \\ f'(\eta) & \theta'(\eta) \end{vmatrix} - A\left(2\theta(\eta) + \frac{1}{2}\eta\theta'(\eta)\right) = 0, \tag{13}$$

with the boundary conditions

$$f(\eta) = f_w, \quad f'(\eta) = 1 + \gamma f''(\eta), \quad \theta(\eta) = 1 + \phi\theta'(\eta), \quad \text{at } \eta = 0, \tag{14}$$

$$f'(\eta) \to 0, \quad \theta(\eta) \to 0, \quad \text{as } \eta \to \infty, \tag{15}$$

where $A = c/a$ is the unsteadiness parameter, $Pr = \nu/\alpha$ is the Prandtl number, $f_w = -v_0/\sqrt{\nu a}$ is the velocity ratio parameter, $\phi = M\sqrt{a/\nu}$ is the dimensionless thermal slip parameter and $\gamma = L\sqrt{a\nu}$ is the dimensionless velocity slip parameter.

The physical quantities of interest in this study, are skin friction coefficient C_f and local Nusselt number Nu_x, which are defined as

$$C_f = \frac{\tau_w}{\rho u_w^2/2}\,, \qquad Nu_x = \frac{x q_w}{k(T_w - T_\infty)}\,, \tag{16}$$

where τ_w is the skin fraction and q_w is the heat transfer from the sheet and are given by

$$\tau_w = \mu \left.\frac{\partial u}{\partial y}\right|_{y=0}, \qquad q_w = -k \left.\frac{\partial T}{\partial y}\right|_{y=0}. \tag{17}$$

Here, μ is the dynamic viscosity and k is the thermal conductivity. Using (9) and substituting (17) into (16), we have

$$\frac{1}{2} C_f Re_x^{1/2} = f''(0), \qquad Nu_x/Re_x^{1/2} = -\theta'(0), \tag{18}$$

where $Re_x = u_w x/\nu$ is the local Reynolds number.

3 Preliminaries and notations

In this section, we introduce some properties and mathematical preliminaries on Bernstein polynomials, orthogonal Bernstein polynomials and rational Bernstein functions.

3.1 Bernstein polynomials and their properties

Bernstein polynomials of the degree n are defined on the interval $[a, b]$ as [30]

$$B_{i,n}(x) = \binom{n}{i} \frac{(x-a)^i (b-x)^{n-i}}{(b-a)^n}, \quad 0 \le i \le n, \tag{19}$$

where the binomial coefficients are calculated by $\binom{n}{i} = \frac{n!}{i!(n-i)!}$. These polynomials form a basis on $[a, b]$ and there are $n+1$, n-th-degree polynomials. If $i < 0$ or $i > n$ we set $B_{i,n}(x) = 0$. The properties of Bernstein polynomials have been investigated by many authors, some of which are mentioned briefly here.

a) *The positivity property*:
For all $i = 0, 1, \ldots, n$ and all x in $[a, b]$, we have $B_{i,n}(x) \ge 0$.

b) *The partition of unity property*:
The binomial expansion of the right-hand side of the equality $(b-a)^n = ((x-a) + (b-x))^n$ shows that the sum of all Bernstein polynomials of the degree n is the constant 1, *i.e.*, $\sum_{i=0}^{n} B_{i,n}(x) = 1$.

c) *Recurrence formula*:
These polynomials can be generated by a recursive definition over the interval $[a, b]$ as follows:

$$B_{i,n}(x) = \frac{b-x}{b-a} B_{i,n-1}(x) + \frac{x-a}{b-a} B_{i-1,n-1}(x). \tag{20}$$

d) *Derivative formula*:
An explicit expression for the derivatives of Bernstein polynomials of any degree and any order in terms of Bernstein polynomials on $[0, 1]$, introduced by Doha *et al.* [33] is as follows:

$$\frac{\mathrm{d}^k}{\mathrm{d}x^k} B_{i,n}(x) = \frac{n!}{(n-k)!} \sum_{j=max\{0,i+k-n\}}^{min\{i,k\}} (-1)^{j+k} \binom{k}{j} B_{i-j,n-k}(x). \tag{21}$$

It can easily be shown that for Bernstein polynomials on $[a, b]$ [25]

$$\frac{\mathrm{d}^k}{\mathrm{d}x^k} B_{i,n}(x) = \frac{1}{(b-a)^k} \frac{n!}{(n-k)!} \sum_{j=max\{0,i+k-n\}}^{min\{i,k\}} (-1)^{j+k} \binom{k}{j} B_{i-j,n-k}(x). \tag{22}$$

e) *The product property*:
The product of two Bernstein polynomials is also a Bernstein polynomial which is given by

$$B_{i,j}(x) B_{k,m}(x) = \frac{\binom{j}{i}\binom{m}{k}}{\binom{j+m}{i+k}} B_{i+k,j+m}(x). \tag{23}$$

f) *The integral properties*:
All Bernstein polynomials of the same order have the same definite integral over the interval $[a, b]$, namely

$$\int_a^b B_{i,n}(x)\mathrm{d}x = \frac{b-a}{n+1}. \tag{24}$$

In addition, the definite integrals of the products of Bernstein polynomials can be found using (23) and (24), as follows:

$$\int_a^b B_{k,n}(x) B_{i,n}(x)\mathrm{d}x = \frac{\binom{n}{k}\binom{n}{i}}{(2n+1)\binom{2n}{k+i}} (b-a). \tag{25}$$

One of the benefits of the Bernstein polynomial approximation of a continuous function f is that it approximates f on $[a, b]$ using only the values of f at $x_i = a + (b-a)i/n$, $i = 0, 1, \ldots, n$, that is,

$$f(x) \simeq \mathbb{B}_n f(x) = \sum_{i=0}^{n} f(x_i) B_{i,n}(x).$$

The above approximation is preferred when the evaluation of f is difficult, expensive and time consuming.

3.2 Orthogonal Bernstein polynomials

The explicit representation of the orthonormal Bernstein polynomials of n-th degree are defined on the interval $[0,1]$ as follows [41]:

$$\mathfrak{B}_{i,n}(x)=\left(\sqrt{2(n-i)+1}\right)(1-x)^{n-i}\sum_{j=0}^{i}(-1)^j\binom{2n+1-j}{i-j}\binom{i}{j}x^{i-j}. \tag{26}$$

Moreover, using (19) on the interval $[0,1]$, (26) can be written in a simpler form in terms of the non-orthonormal Bernstein basis functions as [41]

$$\mathfrak{B}_{i,n}(x)=\left(\sqrt{2(n-i)+1}\right)\sum_{j=0}^{i}(-1)^j\frac{\binom{2n+1-j}{i-j}\binom{i}{j}}{\binom{n-j}{i-j}}B_{i-j,n-j}(x). \tag{27}$$

By changing the variable $x=(t-a)/(b-a)$, we will have the orthonormal Bernstein polynomials on the arbitrary interval $[a,b]$ as

$$\mathfrak{B}_{i,n}(t)=\left(\sqrt{\frac{2(n-i)+1}{b-a}}\right)\sum_{j=0}^{i}(-1)^j\frac{\binom{2n+1-j}{i-j}\binom{i}{j}}{\binom{n-j}{i-j}}B_{i-j,n-j}\left(\frac{t-a}{b-a}\right). \tag{28}$$

The orthonormal Bernstein polynomial, $\mathfrak{B}_{j,n}(x)$ on $[0,1]$ is the n-th eigenfunction of the singular Sturm-Liouville problem [41]

$$\frac{\mathrm{d}}{\mathrm{d}x}\left[x(1-x)^2\frac{\mathrm{d}\mathfrak{B}(x)}{\mathrm{d}x}\right]+n(n+2)(1-x)\mathfrak{B}(x)+(n-j+1)(j-n)\mathfrak{B}(x)=0, \tag{29}$$

with the orthogonality property

$$\int_0^1\mathfrak{B}_{i,n}(x)\mathfrak{B}_{j,n}(x)\mathrm{d}x=\delta_{ij}, \tag{30}$$

where δ_{ij} is the Kronecker delta function. Also, using (28) and (25), the orthonormal polynomials satisfy the following relationships over the interval $[0,1]$

$$\int_0^1\mathfrak{B}_{i,n}(x)B_{j,n}(x)\mathrm{d}x=\begin{cases}\sqrt{(2(n-i)+1)}\displaystyle\sum_{k=0}^{i}(-1)^k\frac{\binom{2n+1-k}{i-k}\binom{i}{k}\binom{n}{j}}{[2n+1-k]\binom{2n-k}{i+j-k}}, & j\geq i,\\ 0, & j<i.\end{cases} \tag{31}$$

In the end of this section, we will prove the following theorem, for the derivatives of $\mathfrak{B}_{i,n}(x)$ at the end points of the interval $[a,b]$.

Theorem 1. *For $k=0,1,\cdots,n$, we have*

$$\frac{\mathrm{d}^k}{\mathrm{d}x^k}\mathfrak{B}_{i,n}(a)=\sqrt{\frac{2(n-i)+1}{(b-a)^{2k+1}}}\sum_{j=0}^{i}\frac{(-1)^{i+k}\binom{2n+1-j}{i-j}\binom{i}{j}\binom{k}{i-j}(n-j)!}{\binom{n-j}{i-j}(n-j-k)!}\gamma_{i-j,k} \tag{32}$$

and

$$\frac{\mathrm{d}^k}{\mathrm{d}x^k}\mathfrak{B}_{i,n}(b)=\sqrt{\frac{2(n-i)+1}{(b-a)^{2k+1}}}\sum_{j=0}^{i}\frac{(-1)^{n-i+j}\binom{2n+1-j}{i-j}\binom{i}{j}\binom{k}{n-i}(n-j)!}{\binom{n-j}{i-j}(n-j-k)!}\gamma_{n-i,k}, \tag{33}$$

where

$$\gamma_{i,k}=\begin{cases}1, & i\leq k,\\ 0, & i>k.\end{cases} \tag{34}$$

Proof. For a fixed value of k if $i=0,1,\cdots,k$, then $\min\{i,k\}=i$. Moreover $B_{0,n}(a)=1$ and $B_{i,n}(a)=0$, $i=1,2,\cdots,n$. So, from (22), we can get $j\leq i$ and

$$\frac{\mathrm{d}^k}{\mathrm{d}x^k}B_{i,n}(a)=\frac{(-1)^{i+k}}{(b-a)^k}\frac{n!}{(n-k)!}\binom{k}{i}. \tag{35}$$

Also, if $i=k+1,k+2,\cdots,n$, then $\min\{i,k\}=k$. So, from (22), we can get $j<i$ and $\frac{\mathrm{d}^k}{\mathrm{d}x^k}B_{i,n}(a)=0$. Thus we have

$$\frac{\mathrm{d}^k}{\mathrm{d}x^k}B_{i,n}(a)=\frac{(-1)^{i+k}}{(b-a)^k}\frac{n!}{(n-k)!}\binom{k}{i}\gamma_{i,k}. \tag{36}$$

Similarly, it can be easily shown that, for $x = b$,

$$\frac{\mathrm{d}^k}{\mathrm{d}x^k} B_{i,n}(b) = \frac{(-1)^{n-i}}{(b-a)^k} \frac{n!}{(n-k)!} \binom{k}{n-i} \gamma_{n-i,k}. \tag{37}$$

Using (28), we can write

$$\frac{\mathrm{d}^k}{\mathrm{d}x^k} \mathfrak{B}_{i,n}(x) = \left(\sqrt{\frac{2(n-i)+1}{b-a}} \right) \sum_{j=0}^{i} (-1)^j \frac{\binom{2n+1-j}{i-j}\binom{i}{j}}{\binom{n-j}{i-j}} \frac{\mathrm{d}^k}{\mathrm{d}x^k} B_{i-j,n-j}(x). \tag{38}$$

Therefore from (36)–(38) we have

$$\frac{\mathrm{d}^k}{\mathrm{d}x^k} \mathfrak{B}_{i,n}(a) = \left(\sqrt{\frac{2(n-i)+1}{b-a}} \right) \sum_{j=0}^{i} (-1)^j \frac{\binom{2n+1-j}{i-j}\binom{i}{j}}{\binom{n-j}{i-j}} \frac{(-1)^{i-j+k}(n-j)!\binom{k}{i-j}}{(b-a)^k (n-j-k)!} \gamma_{i-j,k},$$

$$\frac{\mathrm{d}^k}{\mathrm{d}x^k} \mathfrak{B}_{i,n}(b) = \left(\sqrt{\frac{2(n-i)+1}{b-a}} \right) \sum_{j=0}^{i} (-1)^j \frac{\binom{2n+1-j}{i-j}\binom{i}{j}}{\binom{n-j}{i-j}} \frac{(-1)^{n-i}(n-j)!\binom{k}{n-i}}{(b-a)^k (n-j-k)!} \gamma_{n-i,k}. \qquad \square$$

3.3 Rational Bernstein functions (RBFs)

Many science and engineering problems of current interest are set in unbounded domains. The use of a suitable mapping to transfer semi-infinite domain $[0, +\infty)$ to the finite domain $[a, b]$ is a common and effective strategy to construct approximations on the half line. In this section we describe the rational Bernstein functions (RBFs) and express some of their basic properties and asymptotic behaviors for solving differential equations on the half-line.

3.3.1 Basic properties

We define the rational Bernstein functions (RBFs) of order n as follows:

$$\mathbf{RB}_{i,n}(x; l) = \mathfrak{B}_{i,n}(\Phi_l(x)), \quad i = 0, 1, \ldots, n, \tag{39}$$

where $\Phi_l = [0, +\infty) \to [a, b)$ is an algebraic mapping given by

$$\Phi_l(x) = \frac{bx + al}{x + l}, \tag{40}$$

and l is a positive scaling/stretching factor. The inverse mapping of $y = \Phi_l(x)$ is

$$x = \Phi_l^{-1}(y) = \frac{l(y-a)}{b-y}. \tag{41}$$

Furthermore, we can find the inverse image of the spaced nodes $\{y_j\}_{j=0}^n \subset [a, b)$ as

$$x_j^l = \Phi_l^{-1}(y_j) = \frac{l(y_j - a)}{b - y_j}, \quad j = 0, 1, \ldots, n. \tag{42}$$

Theorem 2. *Let $a = 0$ and $b = 1$, then the rational Bernstein functions $\mathbf{RB}_{j,n}(y; l)$ on $[0, \infty)$ are the eigenfunctions of the singular Sturm-Liouville problem:*

$$y(y+l)\frac{\mathrm{d}^2 p(y)}{\mathrm{d}y^2} + l\frac{\mathrm{d}p(y)}{\mathrm{d}y} + n(n+2)\left(\frac{l}{y+l}\right) p(y) + \gamma_{j,n} p(y) = 0, \tag{43}$$

where $\gamma_{j,n} = (n - j + 1)(j - n), j = 0, 1, \ldots, n$.

Proof. As mentioned in sect. 3, $\mathfrak{B}_{j,n}(x)$ on $[0,1]$ is the n-th eigenfunction of the singular Sturm-Liouville problem (29). Let

$$p(y) = \bar{\mathfrak{B}}_{j,n}\left(\frac{y}{y+l}\right). \tag{44}$$

Now by using the following transformations:

$$x = \frac{y}{y+l}, \quad y = \frac{lx}{1-x}, \quad x \in [0,1),\ y \in [0,\infty), \tag{45}$$

we can get

$$\frac{\mathrm{d}\mathfrak{B}_{j,n}(x)}{\mathrm{d}x} = \frac{l}{(1-x)^2}\frac{\mathrm{d}p(y)}{\mathrm{d}y}, \qquad \frac{\mathrm{d}}{\mathrm{d}x}\left(\frac{\mathrm{d}p(y)}{\mathrm{d}y}\right) = \frac{l}{(1-x)^2}\frac{\mathrm{d}^2p(y)}{\mathrm{d}y^2}. \tag{46}$$

Inserting (46) into (29), yields

$$l\left[\frac{\mathrm{d}p(y)}{\mathrm{d}y} + \frac{lx}{(1-x)^2}\frac{\mathrm{d}^2p(y)}{\mathrm{d}y^2}\right] + n(n+2)(1-x)p(y) + \gamma_{j,n}p(y) = 0, \tag{47}$$

where $\gamma_{j,n} = (n-j+1)(j-n), j = 0,1,\ldots,n$. Consequently, from (45) and (47), the Sturm-Liouville problem for the rational Bernstein functions can be derived as (43). □

Lemma 1. *For $i = 0,1,\cdots,n$, we have:*

$$1)\quad \mathbf{RB}_{i,n}(0;l) = (-1)^i\sqrt{\frac{2(n-i)+1}{b-a}}, \tag{48}$$

$$2)\quad \lim_{x\to+\infty}\mathbf{RB}_{i,n}(x;l) = \begin{cases} 0, & 0 \le i \le n-1, \\ \dfrac{1}{\sqrt{b-a}}\displaystyle\sum_{j=0}^{n}(-1)^j\binom{2n+1-j}{n-j}\binom{n}{j}, & i = n, \end{cases} \tag{49}$$

$$3)\quad \mathbf{RB}'_{i,n}(0;l) = \left(\sqrt{\frac{2(n-i)+1}{l^2(b-a)}}\right)(-1)^{i+1}(-i^2+2in+i+n), \tag{50}$$

$$4)\quad \lim_{x\to+\infty}\mathbf{RB}'_{i,n}(x;l) = 0, \tag{51}$$

$$5)\quad \mathbf{RB}''_{i,n}(0;l) = \frac{-2(b-a)}{l^2}\mathbf{RB}'_{i,n}(0;l) + \sqrt{\frac{2(n-i)+1}{4l^4(b-a)}}(-1)^i\chi_{n,i}, \tag{52}$$

where $\chi_{n,i} = 2ni(i^2 - 2\,in - i - 2\,n + 4)(i - 2\,n - 1)(n-1)$.

Proof. From (39), we have

$$\begin{aligned}
&\mathbf{RB}_{i,n}(x;l) = \mathfrak{B}_{i,n}(\Phi_l(x)),\\
&\mathbf{RB}'_{i,n}(x;l) = \Phi'_l(x)\mathfrak{B}'_{i,n}(\Phi_l(x)),\\
&\mathbf{RB}''_{i,n}(x;l) = \Phi''_l(x)\mathfrak{B}'_{i,n}(\Phi_l(x)) + \Phi'_l(x)^2\mathfrak{B}''_{i,n}(\Phi_l(x)).
\end{aligned}$$

In addition, from (40) it follows that

$$\begin{aligned}
\Phi_l(0) &= a,\\
\lim_{x\to+\infty}\Phi_l(x) &= b,\\
\Phi'_l(0) &= \frac{b-a}{l},\\
\lim_{x\to+\infty}\Phi'_l(x) &= 0,\\
\Phi''_l(0) &= \frac{-2(b-a)}{l^2}.
\end{aligned}$$

Now, by applying theorem 1 in the special cases $k = 0,1,2$, the lemma can be proved. □

Remark 1. Boyd in [42, 43] offered guidelines for optimizing the map parameter l for rational Chebyshev functions, which is useful for the presented method in this paper, too. For the map parameter l we have the following results:

- In general, there is no way to avoid a small amount of trial and error in choosing l when solving problems on an infinite domain.
- The optimum value of l varies with the number of collocation points.
- A little experimentation is usually sufficient to determine a suitable value of l because near the optimum value of l, the accuracy is insensitive to the precise value of l.
- The parameter l is a scaling/stretching factor which can be used to fine tune the spacing of collocation points.

3.3.2 Function approximation

Let us denote $\Lambda = [0, +\infty)$. We determine $w(x) = \frac{l(b-a)}{(x+l)^2}$ as a non-negative, integrable and real-valued weight function for the rational Bernstein functions over the interval $[0, +\infty)$. We define

$$L^2_w(\Lambda) = \{f | f \text{ is measurable on } \Lambda \text{ and } \|f\|_w < \infty\}, \tag{53}$$

equipped with the following inner product and norm:

$$\langle f, g\rangle_w = \int_\Lambda f(x)g(x)w(x)\mathrm{d}x, \qquad \|f\|_w = \langle f, f\rangle_w^{\frac{1}{2}}. \tag{54}$$

Let $y = \Phi_l(x)$, then we have

$$\frac{\mathrm{d}y}{\mathrm{d}x} = \frac{l(b-a)}{(x+l)^2}, \qquad \frac{\mathrm{d}x}{\mathrm{d}y} = \frac{l(b-a)}{(b-y)^2}, \qquad w(x)\frac{\mathrm{d}x}{\mathrm{d}y} = 1. \tag{55}$$

Hence, the orthogonality relation (30) leads to

$$\langle \mathbf{RB}_{i,n}(x; l), \mathbf{RB}_{j,n}(x; l)\rangle_w = \delta_{ij}. \tag{56}$$

Now, suppose that $H = L^2_w(\Lambda)$, and let $\{\mathbf{RB}_{0,n}(x; l), \mathbf{RB}_{1,n}(x; l), \ldots, \mathbf{RB}_{n,n}(x; l)\} \subset H$ be the set of rational orthonormal Bernstein functions of the order n. Also, we define $P^l_n : L^2_w(\Lambda) \longrightarrow \mathfrak{EB}^l_n$ by

$$P^l_n f(x) = \sum_{i=0}^{n} f_i \mathbf{RB}_{i,n}(x; l), \tag{57}$$

where

$$\mathfrak{EB}^l_n = \mathrm{Span}\{\mathbf{RB}_{0,n}(x; l), \mathbf{RB}_{1,n}(x; l), \ldots, \mathbf{RB}_{n,n}(x; l)\}. \tag{58}$$

Theorem 3. [44] *For every given f in a Hilbert space H and every given closed subspace Z of H there is a unique best approximation to w from Z.*

Since $H = L^2_w(\Lambda)$ is Hilbert space and $\mathfrak{EB}^l_n$ is a finite-dimensional subspace and $\mathfrak{EB}^l_n$ is a closed subspace of H, therefore, $\mathfrak{EB}^l_n$ is a complete subspace of H. So, if f be an arbitrary element in H, by theorem 3, f has the unique best approximation from $\mathfrak{EB}^l_n$ such as f^*, that is

$$\exists f^* \in \mathfrak{EB}^l_n; \quad \forall g \in \mathfrak{EB}^l_n \quad \|f - f^*\|_w \leq \|f - g\|_w. \tag{59}$$

Since $f^* \in \mathfrak{EB}^l_n$, there exist the unique coefficients $f_0, f_1, \ldots, f_n$ such that

$$f(x) \simeq f^*(x) = \sum_{i=0}^{n} f_i \mathbf{RB}_{i,n}(x; l), \tag{60}$$

where the coefficients f_i can be obtained by

$$f_i = \langle f(x), \mathbf{RB}_{j,n}(x; l)\rangle_w, \quad i = 0, 1, \ldots, n. \tag{61}$$

4 Rational Bernstein collocation method (RBCM)

In this section, we use the rational Bernstein collocation method (RBCM) to solve the governing nonlinear differential equations for stretching permeable surface in the presence of the velocity slip and temperature jump effects. Consider the system of nonlinear ordinary differential equations (12) and (13) with boundary conditions (14) and (15) to determine the approximate solutions of $f(\eta)$ and $\theta(\eta)$.

At first, we approximate function $f(\eta)$ by (n_f+1) terms of rational Bernstein functions as

$$f(\eta) \simeq P_{n_f}^{l_f} f(\eta) = \sum_{i=0}^{n_f} f_i \mathbf{RB}_{i,n_f}(\eta; l_f). \tag{62}$$

From the fourth part of lemma 1, we have

$$\lim_{\eta\to+\infty} \frac{\mathrm{d}P_{n_f}^{l_f} f(\eta)}{\mathrm{d}\eta} = \sum_{i=0}^{n_f} f_i \left(\lim_{\eta\to+\infty} \mathbf{RB}'_{i,n_f}(\eta; l_f) \right) = 0, \tag{63}$$

and therefore the first boundary condition (15) is satisfied. Now, we construct the residual function $RES_f(\eta)$ by substituting $f(\eta)$ by $P_{n_f}^{l_f} f(\eta)$ in (12) as

$$RES_f(\eta) = \frac{\mathrm{d}^3 P_{n_f}^{l_f} f(\eta)}{\mathrm{d}\eta^3} - \left(\frac{\mathrm{d}P_{n_f}^{l_f} f(\eta)}{\mathrm{d}\eta} \right)^2 + P_{n_f}^{l_f} f(\eta) \frac{\mathrm{d}^2 P_{n_f}^{l_f} f(\eta)}{\mathrm{d}\eta^2} - A \left(\frac{\mathrm{d}P_{n_f}^{l_f} f(\eta)}{\mathrm{d}\eta} + \frac{1}{2}\eta \frac{\mathrm{d}^2 P_{n_f}^{l_f} f(\eta)}{\mathrm{d}\eta^2} \right). \tag{64}$$

Let

$$t_j = -\cos\left(\frac{2j\pi}{2n_f+1} \right), \quad j = 0, 1, \ldots, n_f, \tag{65}$$

be the (n_f+1) Chebyshev-Gauss-Radau points on interval $[-1, 1)$. From (42) with $a = -1$ and $b = 1$, we define the collocation points $\eta_j^{l_f} \in [0, +\infty)$ as follows:

$$\eta_j^{l_f} = \Phi_{l_f}^{-1}(t_j) = \frac{l_f(t_j+1)}{1-t_j}, \quad j = 0, 1, \ldots, n_f. \tag{66}$$

The equations for obtaining the coefficients f_is come from equalizing $RES_f(\eta)$ to zero at collocation points $\{\eta_j^{l_f}\}_{j=0}^{n_f-2}$ plus two no-slip and slip boundary conditions as follows:

$$RES_f(\eta_j^{l_f}) = 0, \quad j = 0, 1, \ldots, n_f - 2, \tag{67}$$

$$P_{n_f}^{l_f} f(\eta_0^{l_f}) = f_w, \qquad \frac{\mathrm{d}P_{n_f}^{l_f} f(\eta)}{\mathrm{d}\eta}\bigg|_{\eta=\eta_0^{l_f}} = 1 + \gamma \frac{\mathrm{d}^2 P_{n_f}^{l_f} f(\eta)}{\mathrm{d}\eta^2}\bigg|_{\eta=\eta_0^{l_f}}. \tag{68}$$

We can rewrite the boundary conditions (68) by the first, third and fifth parts of lemma 1 as

$$\begin{aligned} &\sum_{i=0}^{n_f} f_i \zeta_i^{(1)} = f_w, \\ &\sum_{i=0}^{n_f} f_i \zeta_i^{(2)} = 1 + \gamma \sum_{i=0}^{n_f} f_i \zeta_i^{(3)}, \end{aligned} \tag{69}$$

where

$$\begin{aligned} \zeta_i^{(1)} &= (-1)^i \sqrt{\frac{2(n-i)+1}{b-a}}, \\ \zeta_i^{(2)} &= \left(\sqrt{\frac{2(n-i)+1}{l^2(b-a)}} \right) (-1)^{i+1} (-i^2 + 2in + i + n), \\ \zeta_i^{(3)} &= \frac{-2(b-a)}{l^2} \zeta_i^{(2)} + \sqrt{\frac{2(n-i)+1}{4l^4(b-a)}} (-1)^i \chi_{n,i}. \end{aligned}$$

Equations (67) and (69) generate a set of $(n_f + 1)$ nonlinear equations that can be solved by Newton method for the unknown coefficients f_is.

Now, by finding the approximate solutions $P^{l_f}_{n_f} f(\eta)$, we suppose that the approximate solution $\theta(\eta)$ of (13) is as follows:

$$\theta(\eta) \simeq P^{l_\theta}_{n_\theta}\theta(\eta) = \sum_{i=0}^{n_\theta} \theta_i \mathbf{RB}_{i,n_\theta}(\eta; l_\theta). \tag{70}$$

Similarly, we make the residual function $RES_\theta(\eta)$ by substituting $P^{l_\theta}_{n_\theta}\theta(\eta)$ in equation (13) as:

$$RES_\theta(\eta) = \frac{1}{Pr}\frac{\mathrm{d}^2 P^{l_\theta}_{n_\theta}\theta(\eta)}{\mathrm{d}\eta^2} + \begin{vmatrix} P^{l_f}_{n_f} f(\eta) & P^{l_\theta}_{n_\theta}\theta(\eta) \\ \dfrac{\mathrm{d}P^{l_f}_{n_f} f(\eta)}{\mathrm{d}\eta} & \dfrac{\mathrm{d}P^{l_\theta}_{n_\theta}\theta(\eta)}{\mathrm{d}\eta} \end{vmatrix} - A\left(2P^{l_\theta}_{n_\theta}\theta(\eta) + \frac{1}{2}\eta\frac{\mathrm{d}P^{l_\theta}_{n_\theta}\theta(\eta)}{\mathrm{d}\eta}\right) = 0. \tag{71}$$

Using the collocation points (66), the equations for obtaining the coefficients θ_is come through equalizing $RES_\theta(\eta)$ to zero at these points plus two no-slip and slip boundary conditions as follows:

$$RES_\theta(\eta^{l_\theta}_j) = 0, \quad j = 0, 1, \ldots, n_\theta - 2, \tag{72}$$

$$P^{l_\theta}_{n_\theta}\theta(\eta^{l_\theta}_0) = 1 + \phi\frac{\mathrm{d}P^{l_\theta}_{n_\theta}\theta(\eta)}{\mathrm{d}\eta}\bigg|_{\eta=\eta^{l_\theta}_0}, \qquad \lim_{\eta\to+\infty} P^{l_\theta}_{n_\theta}\theta(\eta) = 0. \tag{73}$$

Again, by the first and three parts of lemma 1, we rewrite the boundary conditions (73) as follows:

$$\sum_{i=0}^{n_\theta}\theta_i\zeta^{(1)}_i = 1 + \phi\sum_{i=0}^{n_\theta}\theta_i\zeta^{(2)}_i, \quad \theta_{n_\theta} = 0. \tag{74}$$

Equations (72) and (74) generate a set of $(n_\theta + 1)$ nonlinear equations that can be solved by Newton method for the unknown coefficients θ_is.

5 Results and discussion

In this section, we present the numerical results of the RBCM to solve the system of nonlinear ordinary differential equations (12) and (13) subject to boundary conditions (14) and (15). A parametric study is presented to see the influence of the unsteadiness parameter, Prandtl number, suction parameter, velocity slip parameter and thermal slip parameter on the fluid velocity component and temperature distribution profiles. To illustrate the reliability of the proposed method, we compare the numerical results of RBCM with the other researcher's result and numerical method based on fourth-order Runge-Kutta method along with shooting technique.

To evaluate the validity and applicability of the presented technique, we define the following absolute errors:

$$E_{f'}(\eta_k) = |f'_{RBCM}(\eta_k) - f'_{Rk4}(\eta_k)|, \quad E_\theta(\eta_k) = |\theta_{RBCM}(\eta_k) - \theta_{Rk4}(\eta_k)|, \quad \eta_k \in [a, b], \tag{75}$$

where $\eta_k = a + \frac{i(b-a)}{N}$, $i = 0, 1, \ldots, N$. Figure 2 gives a comparison between the present RBCM results and the fourth-order Runge-Kutta (RK4) method along with shooting technique for some parameters of A, Pr, f_w, ϕ, γ with $N = 100$.

Figure 3 shows the velocity and temperature distributions for different value of unsteadiness parameter A. It is clearly observed that the velocity and temperature profiles decrease with increasing the value of A. The temperature profiles for different value of the Prandtl number are depicted in fig. 4. It is observed that an increase in the value of Prandtl number decreases the thermal boundary layer thickness. It is evident that the lower value of Pr gives the higher temperature and thermal boundary layer thickness. Figure 5 illustrates the effect of suction parameter f_w on the velocity and temperature. It is seen that with increasing of f_w the velocity and temperature profile go to boundary values in the smaller quantities of perpendicular distance, η. The influence of the velocity slip parameter γ on the velocity and temperature profiles is shown in fig. 6. The value of γ changes from 0 to 5, where $\gamma = 0$ indicates the no-slip condition. It is clearly observed that the velocity profile decreases with increasing the value of γ, whereas the temperature distribution increases. The effect of γ on the temperature distribution in contrast to velocity profile is far less clear. Figure 7 illustrates the effect of the thermal slip parameter ϕ on the temperature distribution. It is obvious that with increasing of ϕ, the thermal of the flow decreases. The effects of the suction parameter f_w, velocity slip parameter γ and unsteadiness parameter A on the skin friction coefficient are displayed in fig. 8. As can be seen,

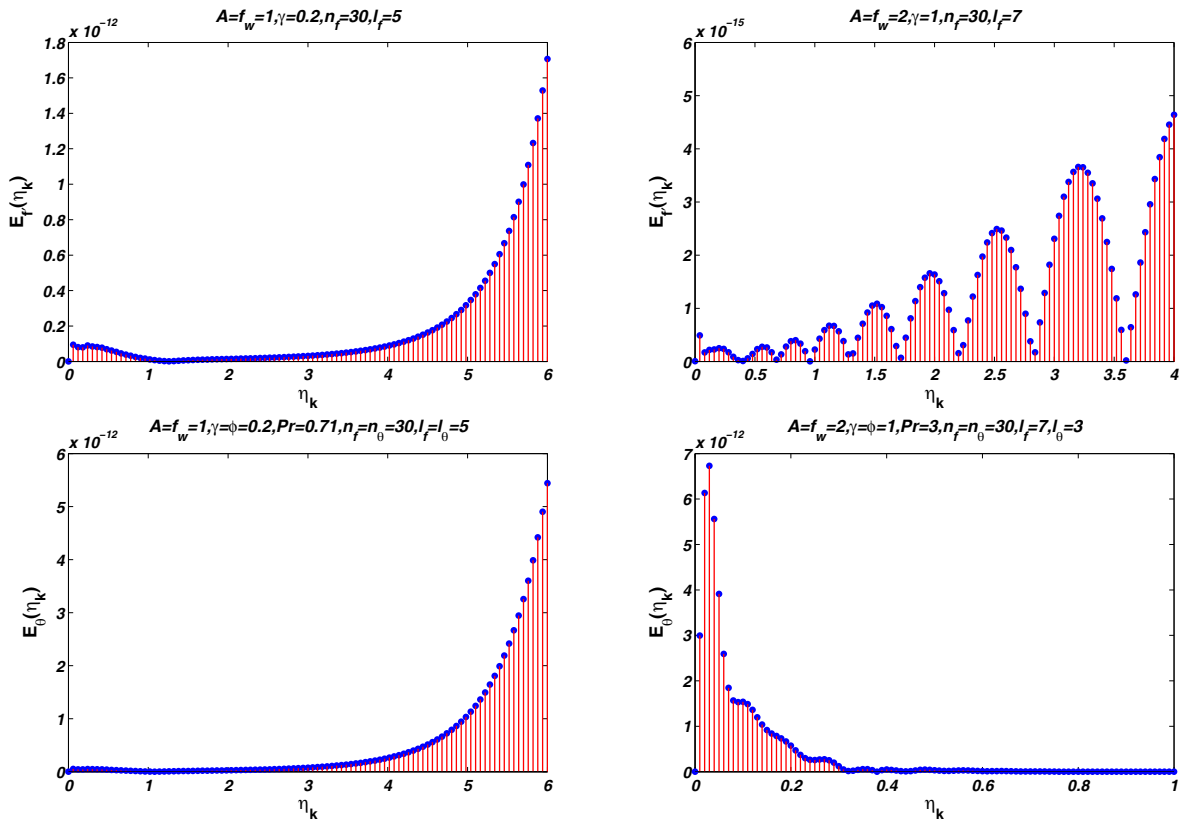

Fig. 2. Plots of error values $E_{f'}(\eta_k)$ and $E_\theta(\eta_k)$ with $N = 100$.

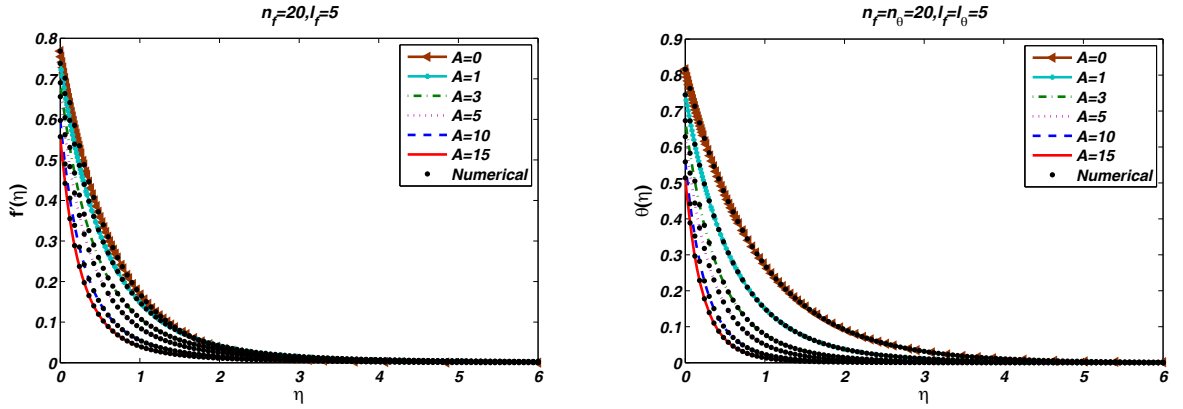

Fig. 3. Effect of the unsteadiness parameter A on the velocity and temperature profiles with $Pr = 0.71$, $f_w = 1$, $\phi = \gamma = 0.2$.

by increasing the f_w and A, that skin friction coefficient decreases. Moreover, the skin friction coefficient increases with the increasing velocity slip parameter γ. Also, it is clear that large values of γ, A and f_w have a negligible effect in the skin friction coefficient. Figure 9 shows the graphical representations for the various values of A, f_w, Pr, ϕ on the local Nusselt number. It is observed that an increase in A and f_w increases the local Nusselt number. It is clear that increasing Pr enhances the local Nusselt number for the small values of ϕ. We also validate our method by comparing the skin friction coefficient and the local Nusselt number with the available results in the literature, as shown in tables 1 and 2. The evaluated errors and CPU times denote the accuracy and efficiency of the new proposed method.

Although some methods to choose the map parameter l for different problem are suggested in [42,43], there is not a general method for this choice and it is usually selected by trial and error. However, we need to choose the parameter l so that it controls the width of the base functions. Here, we introduce the following method for finding a suitable map parameter l.

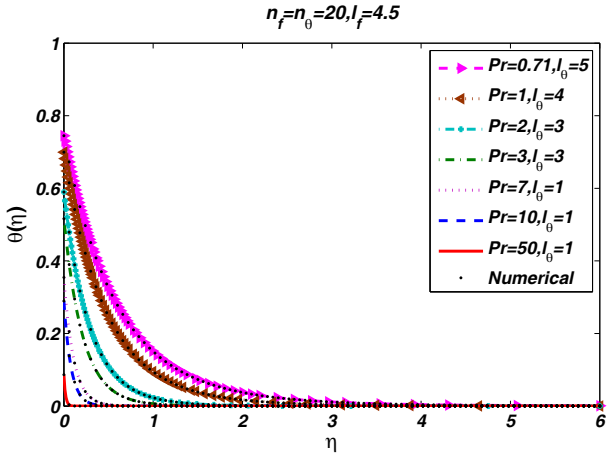

Fig. 4. Effect of the Prandtl number Pr on the temperature profile with $A = f_w = 1$, $\phi = \gamma = 0.2$.

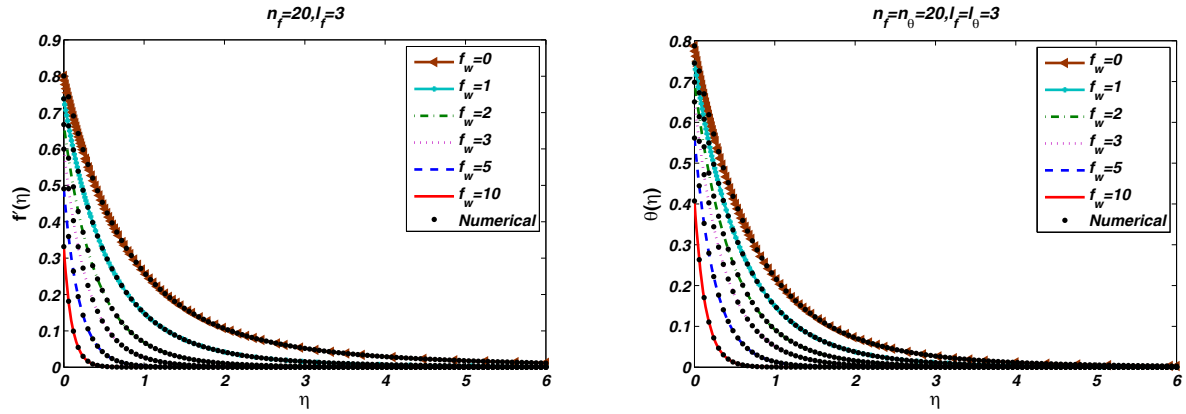

Fig. 5. Effect of the suction parameter f_w on the velocity and temperature profiles with $Pr = 0.71$, $A = 1$, $\phi = \gamma = 0.2$.

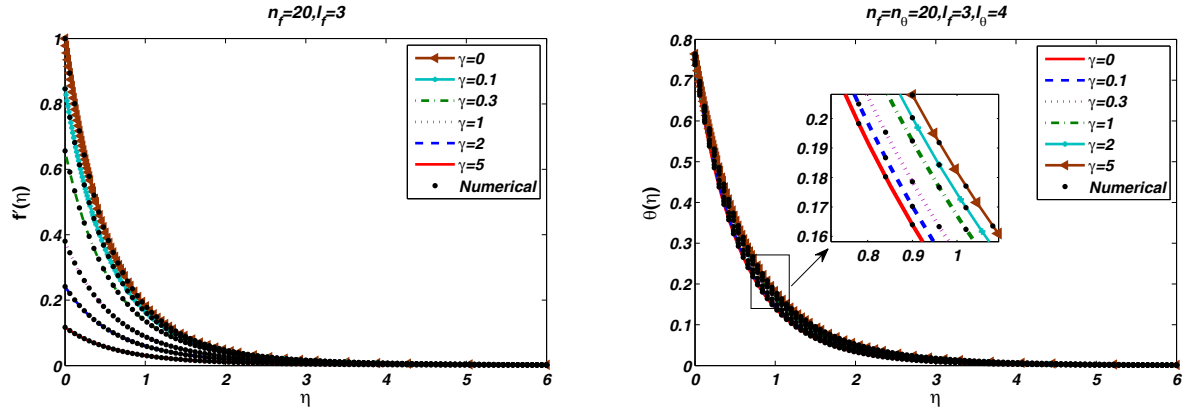

Fig. 6. Effect of the velocity slips parameter γ on the velocity and temperature profiles with $Pr = 0.71$, $A = f_w = 1$, $\phi = 0.2$.

In this method, we depict the maximum absolute residual error *versus* l for a fixed values of n. This curve has a "V" shape. for reasons explained in more detail in [42, 43, 45].

Figure 10 shows the graphs of maximum absolute residual errors (64) and (71) for case $A = 3$, $f_w = 1$, $Pr = 0.71$, $\gamma = \phi = 0.2$ with $n_f = n_\theta = 10, 20, 30$ and various values of l_f, l_θ. We observe that the optimum values of parameter l_f are about $l_f = 3, 3.5$ and 3.7 for $n_f = 10, 20$ and 30, respectively. Also, we can see that the optimum values of parameter l_θ are about $l_\theta = 3, 3.5$ and 4 for $n_\theta = 10, 20$ and 30, respectively.

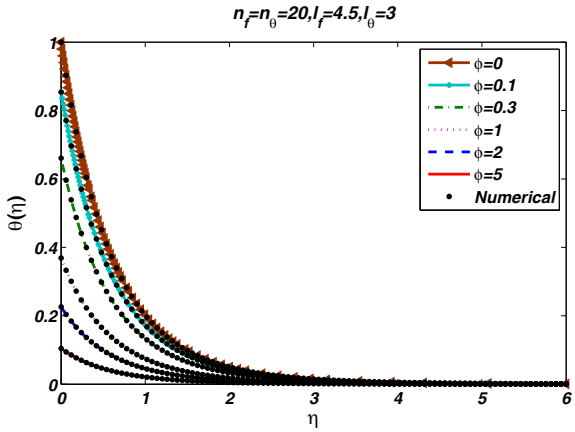

Fig. 7. Effect of the thermal slip parameter ϕ on the temperature profile with $Pr = 0.71$, $A = f_w = 1$, $\gamma = 0.2$.

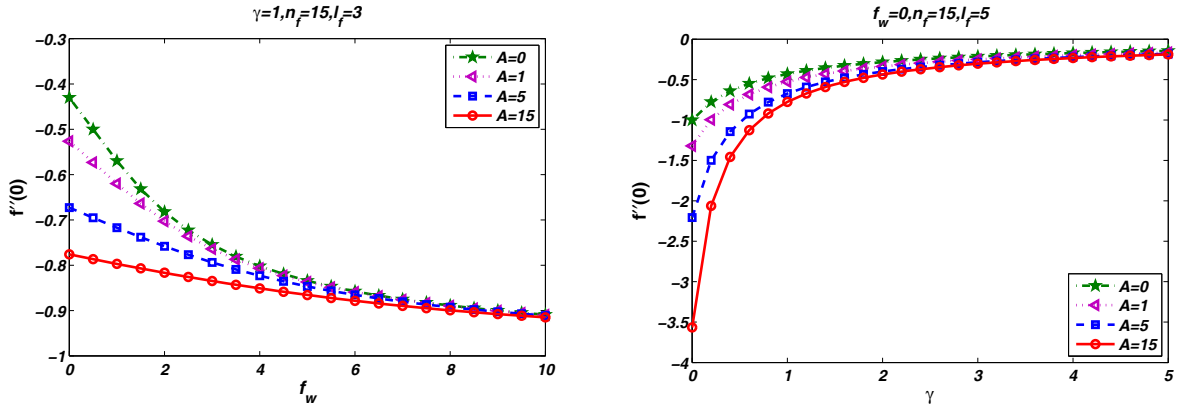

Fig. 8. Variation of the skin friction coefficient $f''(0)$.

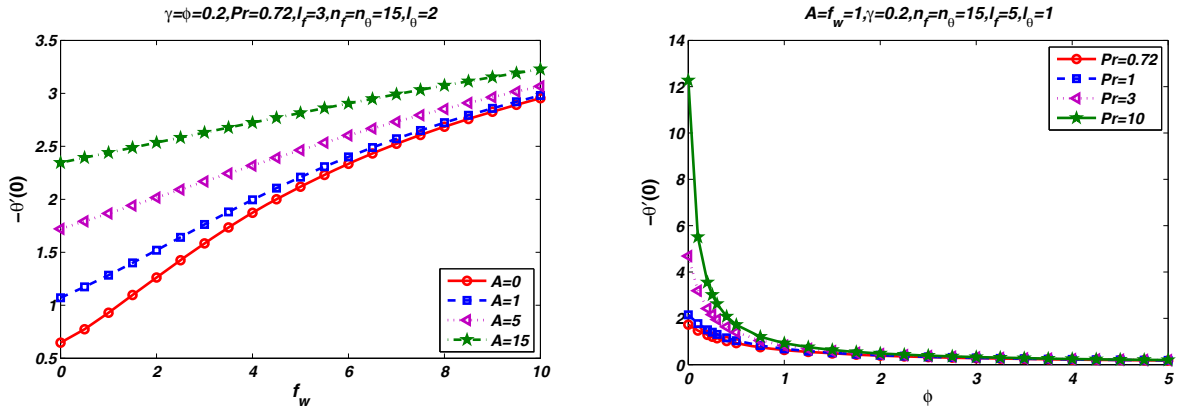

Fig. 9. Variation of the local Nusselt number $-\theta'(0)$.

6 Conclusions

In this study, the velocity slip and temperature jump effects for an unsteady flow past a porous accelerating stretching surface was investigated using the rational Bernstein collocation method (RBCM). The difficulty in this type of problems, due to the existence of its slip boundary conditions, was overcome here. The effects of various parameters like the unsteadiness parameter A, Prandtl number Pr, suction parameter f_w, velocity slip parameter γ and thermal slip parameter ϕ on the velocity and temperature distribution profiles are discussed with the help of graphs. The effect of the parameters on the skin friction and the local Nusselt number is also examined. The results obtained from RBCM are in excellent agreement with those obtained from numerical solutions by fourth-order Runge-Kutta method and other previous methods.

Table 1. Comparison results of $-f''(0)$ for various values of A, f_w, γ with $n_f = 30$.

A	γ	f_w	l_f	RBCM	CPU time(s)	RK4	Error
0	0	0	7	1.00000000	8.36	1.00000000	$7.47128740e-10$
	2	5	3	0.45469419	9.64	0.45469419	$4.38975174e-13$
	5	10	3	0.19607918	9.82	0.19607918	$3.06171982e-13$
1	0	0	7	1.32052206	10.86	1.32052206	$1.23484110e-16$
	2	5	3	0.45549392	11.73	0.45549392	$9.47656554e-17$
	5	10	3	0.19609829	13.21	0.19609829	$4.27606791e-17$
7	0	0	3	2.53708081	11.14	2.53708081	$6.33748846e-20$
	2	5	1	0.45974146	13.03	0.45974146	$6.57661674e-14$
	5	10	1	0.19620917	13.85	0.19620917	$1.63879225e-15$
15	0	0	3	3.56613202	12.91	3.56613202	$1.31476036e-18$
	2	5	1	0.46401671	14.37	0.46401671	$8.62994603e-17$
	5	10	1	0.19634753	14.98	0.19634753	$3.53598317e-16$

Table 2. Comparison results of $-\theta'(0)$ for various values of A, f_w, γ, Pr, ϕ with $n_f = n_\theta = 30$.

A	γ	f_w	ϕ	Pr	l_f	l_θ	Ref. [46]	Ref. [47]	Ref. [48]	Ref. [49]	Ref. [40]	RBCM	RK4	Error
0	0	0	0	0.72	7	8.2	0.8058	0.8086	0.8086	0.80868	0.80863135	0.80863140	0.80863134	$8.92268800e-09$
				1	7	7.2	0.9961	1.0000	1.0000		1.00000000	1.00000000	1.00000000	$4.77407300e-09$
				10	7	1	3.7006	3.7207	3.7207			3.72064063	3.72067116	$3.05267526e-05$
				100	7	0.55		12.2941	12.2940	12.2940		12.2940911	12.2940811	$1.01156526e-05$
1	0	0	0	0.72	7	8						1.41358702	1.41358702	$9.62339619e-16$
				1	7	7		1.6820				1.68199253	1.68199253	$1.64811127e-17$
				10	7	1						5.56377330	5.56377330	$3.70543764e-15$
				100	7	0.5						17.9013332	17.9013332	$1.35796486e-12$
	2	5	2	0.72	3	3						0.44315632	0.44315632	$9.47450917e-17$
				1	3	3						0.45693356	0.45693356	$2.87320610e-18$
				10	3	1						0.49508171	0.49508171	$5.44624965e-15$
				100	3	0.5						0.49963801	–	–

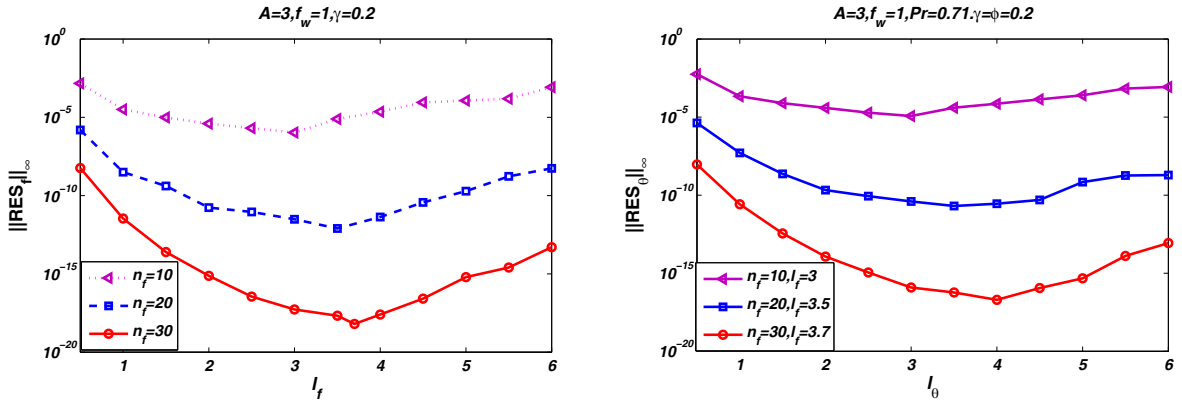

Fig. 10. Comparison of the residual errors for $f(\eta)$ and $\theta(\eta)$ with different choices of the parameters l_f and l_θ and the numbers of grid points n_f and n_θ.

The main advantages of the RBCM are the following:

- The technique is easy to implement and yields very accurate results in comparison with other mentioned methods.
- The proposed method does not require truncating or transforming the semi-infinite domain of the problem to a finite domain.
- This method reduces the solution of the problem to solution of a system of algebraic equations.
- Unlike the Runge-Kutta methods, where provide the solution of the problem at a discrete set of points, the RBCM provides the continuous solution of the problem.

References

1. L.J. Crane, Z. Angew. Math. Phys. **21**, 645 (1970).
2. P.S. Gupta, A.S. Gupta, Can. J. Chem. Eng. **55**, 744 (1977).
3. A. Ishak, R. Nazar, I. Pop, Nonlinear Anal. Real World Appl. **10**, 2909 (2009).
4. M.H. Abolbashari, N. Freidoonimehr, F. Nazari, M.M. Rashidi, Powder Technol. **267**, 256 (2014).
5. M.M. Rashidi, N. Freidoonimehr, A. Hosseini, O.A. Bég, T.K. Hung, Meccanica **49**, 469 (2013).
6. N. Freidoonimehr, M.M. Rashidi, S. Mahmud, Int. J. Therm. Sci. **87**, 136 (2015).
7. J.C. Maxwell, Philos. Trans. R. Soc. London Ser. **170**, 231 (1879).
8. A. Beskok, G.E. Karniadakis, Microscale Thermophys. Eng. **3**, 43 (1999).
9. L.A. Wu, Appl. Phys. Lett. **93**, 253103 (2008).
10. A.K. Srikanth, *Slip flow through long circular tubes*, in *Proceedings of the Sixth International Symposium on Rarefied gas dynamics* (Academic Press, 1969) pp. 667–680.
11. H. Andersson, Acta Mech. **158**, 121 (2002).
12. C.Y. Wang, Chem. Eng. Sci. **57**, 3745 (2002).
13. T.G. Fang, J. Zhang, S.S. Yao, Chin. Phys. Lett. **27**, 124702 (2010).
14. T. Hayat, M. Qasim, S. Mesloub, Int. J. Numer. Methods Fluid. **66**, 963 (2011).
15. S. Jafari, N. Freidoonimehr, J. Braz. Soc. Mech. Sci. Eng. **37**, 1245 (2015).
16. M.H. Abolbashari, N. Freidoonimehr, F. Nazari, M.M. Rashidi, Adv. Powder Technol. **26**, 542 (2015).
17. M. Nawaz, A. Zeeshan, R. Ellahi, S. Abbasbandy, S. Rashidi, Int. J. Numer. Methods Heat Fluid Flow **25**, 665 (2015).
18. A. Zeeshan, A. Majeed, R. Ellahi, J. Mol. Liq. **215**, 549 (2016).
19. A. Majeed, A. Zeeshan, R. Ellahi, J. Mol. Liq. **223**, 528 (2016).
20. K. Maqbool, A. Sohail, N. Manzoor, R. Ellahi, Commun. Theor. Phys. **66**, 547 (2016).
21. R. Ellahi, M.M. Bhatti, I. Pop, Int. J. Numer. Methods Heat Fluid Flow **26**, 1802 (2016).
22. R. Ellahi, F. Hussain, J. Magn. & Magn. Mater. **393**, 284 (2015).
23. P.P. Korovkin, *Interpolation and approximation by polynomials: Bernstein polynomials*, in *Springer Encyclopedia of Mathematics* (Springer, 2001).
24. G. Farin, *Curves and Surfaces for Computer Aided Geometric Design* (Academic Press, Boston, Mass, USA, 1996).
25. M. Heydari, G.B. Loghmani, S.M. Hosseini, Comput. Appl. Math. (2015) DOI: 10.1007/s40314-015-0251-2.
26. D.D. Bhatta, M.I. Bhatti, Appl. Math. Comput. **174**, 1255 (2006).
27. B.N. Mandal, S. Bhattacharya, Appl. Math. Comput. **190**, 1707 (2007).
28. S. Bhattacharya, B.N. Mandal, Appl. Math. Sci. **2**, 1773 (2008).
29. A. Chakrabarti, S.C. Martha, Appl. Math. Comput. **211**, 459 (2009).
30. M.I. Bhatti, P. Bracken, J. Commun. Appl. Math. **205**, 272 (2007).
31. S.A. Yousefi, M. Behroozifar, Int. J. Syst. Sci. **41**, 709 (2010).
32. S.A. Yousefi, M. Behroozifar, M. Dehghan, J. Comput. Appl. Math. **235**, 5272 (2011).
33. E.H. Doha, A.H. Bhrawy, M.A. Saker, Bound. Value Probl. **2011**, 829543 (2011).
34. E.H. Doha, A.H. Bhrawy, M.A. Saker, Appl. Math. Lett. **24**, 559 (2011).
35. S.A. Yousefi, M. Behroozifar, M. Dehghan, Appl. Math. Model. **36**, 945 (2012).
36. K. Maleknejad, E. Hashemizadeh, B. Basirat, Commun. Nonlinear Sci. Numer. Simulat. **17**, 52 (2012).
37. K. Maleknejad, E. Hashemizadeh, R. Ezzati, Commun. Nonlinear Sci. Numer. Simulat. **16**, 647 (2011).
38. D. Rostamy, K. Karimi, Fract. Calc. Appl. Anal. **15**, 556 (2012).
39. M. Heydari, G.B. Loghmani, M.M. Rashidi, S.M. Hosseini, Propulsion Power Res. **4**, 169 (2015).
40. N. Freidoonimehr, M.M. Rashidi, Z. Yang, A. Hajipour, Y. Xiao-Jun, *Velocity slip and temperature jump effects for an unsteady flow over a stretching permeable surface*, to be published in Thermal Science.
41. Michael A. Bellucci, arXiv:1404.2293 (2014).
42. J.P. Boyd, J. Comput. Phys. **45**, 43 (1982).
43. J.P. Boyd, *Chebyshev and Fourier Spectral Methods*, 2nd edition (Dover Publications Inc., Mineola, 2001).
44. E. Kreyszig, *Introductory Functional Analysis with Applications* (Wiley, New York, 1978).
45. J.P. Boyd, J. Comput. Phys. **69**, 112 (1987).
46. M.E. Ali, Heat Mass Transfer **29**, 227 (1994).
47. A. Ishak, R. Nazar, I. Pop, Meccanica **44**, 369 (2009).
48. L.J. Grubka, K.M. Bobba, ASME J. Heat. Transf. **107**, 248 (1985).
49. A. Mahdy, Nucl. Eng. Des. **249**, 248 (2012).